Surface-state conduction of medium-sized nanowires

Katsuyoshi Kobayashi
Department of Physics, Faculty of Science, Ochanomizu University, 2-1-1 Otsuka, Bunkyo-ku, Tokyo 112-8610, Japan
(Received 25 August 2003; revised manuscript received 29 December 2003; published 30 March 2004)

The electrical conduction of medium-sized nanowires are studied theoretically. As an example the conductance of silicon nanowires with facets is calculated using the Landauer formalism. The electrical currents in the energy region of the bulk band gap are localized at the surfaces of the nanowires, which demonstrates highly inhomogeneous current distribution in medium-sized nanowires. In addition there are cases that current distributions are localized along the edges of the nanowires. This is due to the existence of the states localized at the edges of wedges surrounded by two semi-infinite surfaces. The conditions for existence of the edge states are discussed using one-dimensional models. The possibility of vertex states localized at intersections of edge lines is also mentioned.

DOI: 10.1103/PhysRevB.69.115338 PACS number(s): 73.63.Nm, 73.20.At, 73.25.+i, 73.22.Dj

I. INTRODUCTION

We present a theoretical study on the electrical conduction of medium-sized nanowires. Here we mean by medium size the sizes which are larger than the atomic scales and are smaller than the scales where surface effects can be neglected. These ensure that when surface states exist on the surfaces of nanowires, surface states and bulk states are well distinguishable, and their contributions to electrical conduction are comparable. This can lead to highly inhomogeneous current distribution in nanowires, which may affect other physical properties such as local temperature and heat conduction.

Another interest in medium-sized nanowires is the existence of lines, on which different surfaces meet, if the surfaces of nanowires are faceted. The existence of edges may give rise to new properties which are not understood by the simple sum of those of individual surfaces. The importance of edges has already emphasized, for example, in the electrostatic potential and work functions of faceted metal nanowires[1,2] and in the atomic structures of nanowires.[3] In this paper we emphasize it in the context of the electronic structures and conduction properties of medium-sized nanowires. We actually show a possibility of existence of new states localized at the edges of nanowires.

We choose ideal silicon nanowires as model systems that possess surface states. Silicon nanowires have so far studied extensively. Several examples of recent studies are as follows. The silicon nanowires composed of fullerenelike units were proposed by experimental observations and molecular-orbital calculations.[4] The contacts between hydrogen-terminated silicon nanowires and metal electrodes,[5] and the geometric and electronic structures of silicon nanowires with diameters less than 1 nm (Ref. 6) were studied theoretically by density-functional methods. Recently the surface atomic structures and band gaps of hydrogen-terminated silicon nanowires with small diameters were directly observed experimentally,[7] and silicon nanowires with pentagonal cross sections were predicted theoretically.[8] In contrast to these studies, the interest in the present paper is taken in the surface-state conduction of nanowires.

The reason for the choice of the silicon nanowires in the ideal structures without reconstruction is that they are simple systems and the energy regions of the bulk and surface states are well separated. These make it easy to analyze numerical results and provide a clear view on the physics of medium-sized nanowires. The ideal wires are useful as a prototype.

Of course, in order to compare theoretical results directly with experiments, we must at least take account of the surface reconstructions.[9] In addition, in the case of nanowires, the finite-size effect of surfaces on the reconstructions and the atomic structures at edges are not trivial things. For settling these things the geometrical optimization by density-functional calculations is desirable, which will be done in future works.

In this paper the electronic states of the wires are expressed by a tight-binding method. The conductance of electrode-wire-electrode systems is calculated by the Landauer formalism. We find that the current distribution is localized on the surfaces of the nanowires in the energy region of the bulk band gap. The surfaces where localized current flows and the extent of the current distribution vary with bias voltages. In addition some nanowires show the current distribution localized along the edges of the nanowire surfaces. This is due to that the currents are carried by the states localized at the edges and existing outside the energy regions of the bulk and surface bands. The method and results of numerical calculations are shown in Secs. II and III. The conditions for the existence of the edge states are discussed in Sec. IV, where we refer to a possibility of the existence of vertex states which are localized at the vertices of nanoparticles with facets.

II. METHOD OF NUMERICAL CALCULATION

We calculate the conductance of electrode-nanowire-electrode systems. Figure 1 shows the atomic structure of the system mainly discussed in this paper. The nanowire consists of 1380 Si atoms. The atomic positions of the wire are ideal ones of the bulk geometry. The axis and length of the nanowire are the [110] direction and 36.4 Å, respectively. The six sides of the nanowire are $(1\bar{1}1)$, $(\bar{1}\bar{1}\bar{1})$, $(\bar{1}11)$,$(1\bar{1}\bar{1})$, (001), and $(00\bar{1})$ surfaces. The distances between the $(1\bar{1}1)$

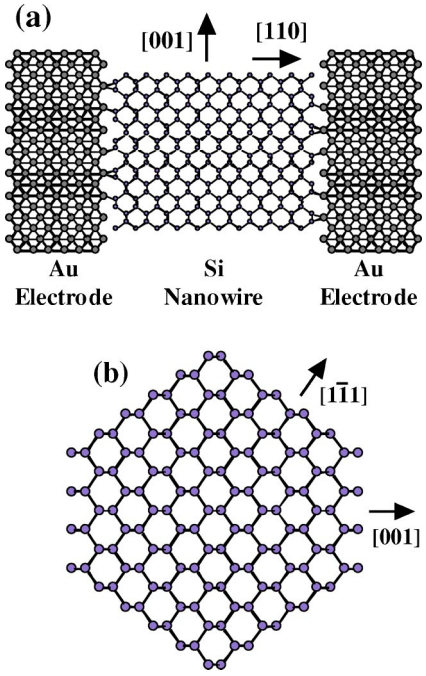

FIG. 1. (a) Top view of a Si nanowire with Au electrodes. (b) Cross section of the Si nanowire. Atoms in different layers are superposed.

and $(\bar{1}1\bar{1})$ surfaces and between the (001) and $(00\bar{1})$ surfaces are 25.4 Å and 28.5 Å, respectively. This type of nanowires may be particularly interesting because their sides are the most fundamental {111} and {001} surfaces of silicon. The small-diameter nanowires experimentally observed are of this type, though their surfaces are terminated with hydrogens.[7]

The electrodes are semi-infinite Au wires. The axis of the Au wires is the [110] direction. The sides of the Au wires are (001), $(00\bar{1})$, $(1\bar{1}0)$, and $(\bar{1}10)$ surfaces. The distances between the (001) and $(00\bar{1})$ surfaces and between the $(1\bar{1}0)$ and $(\bar{1}10)$ surfaces are 36.7 Å and 37.5 Å, respectively. The unit cell of the electrodes consists of 257 atoms.

The distance between the end planes of the Si nanowire and the Au electrodes is 2.38 Å. There are Au atoms at the centers of the end planes of the Au electrodes, but the center axis of the Si nanowire runs midway between the two kinds of atoms nearest to the center. Therefore the shortest distance between Si and Au atoms is 2.47 Å which is a length between the nearest-neighbor Si-Si and Au-Au distances.

The electronic states of the nanowire and electrodes are expressed by tight-binding methods. The sp^3s^* method is used for the Si nanowire,[10] which takes account of $3s$ and $3p$ orbitals and an additional s orbital denoted by s^*. For the Au electrodes and the Au-Si interaction we use the tight-binding parameters by Harrison.[11] The onsite energies of the Au electrodes are adjusted so that the Fermi energy of the Au electrodes is equal to that of the Si nanowire. We neglect the interactions between the s^* orbital of Si and the orbitals of Au.

The conductance is calculated using the Landauer formalism, where conductance is obtained from the transmission probability of the system.[12–14] The method of calculations is similar to previous studies of surface-state conduction.[15–18] The Bloch states of the Au electrodes including evanescent waves are obtained by diagonalizing the transfer matrix defined in terms of the tight-binding Hamiltonian. By imposing the appropriate boundary conditions expressed by the Bloch states on the two Au electrons, the tight-binding Hamiltonian of the electrode-nanowire-electrode system is reduced to a coupled linear equation. The transmission probability is obtained by solving it.

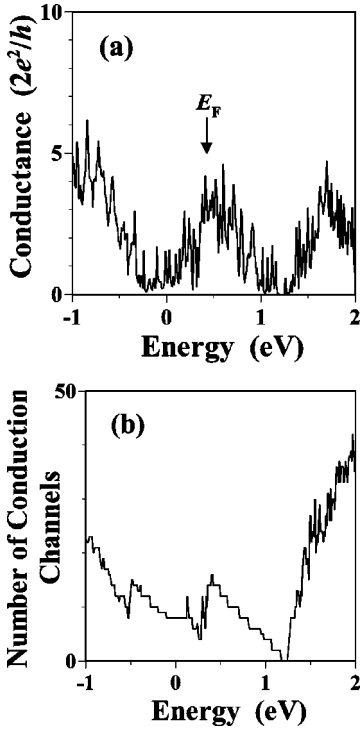

FIG. 2. (a) Conductance spectrum of the Au-Si-Au system shown in Fig. 1. (b) Number of conduction channels of the isolated Si wire.

III. RESULT OF NUMERICAL CALCULATION

Figure 2(a) shows a conductance spectrum of the system shown in Fig. 1. The Fermi energy of the isolated Si nanowire is 0.41 eV, where we define zero in energy as the conduction-band top of bulk silicon in this paper. This definition of energy is convenient to recognize the energy region of the bulk band gap. The conductance spectrum should be shown so that zero in bias voltage corresponds to the Fermi energy. But, for ease of the comparison with band structures, the conductance spectrum is also shown in the units of energy.

Figure 2(b) shows the number of conduction channels of the isolated Si nanowire as a function of energy. The conduction channels are calculated by diagonalizing the transfer matrix for the isolated nanowire. The number of right-going propagating channels is counted. If the contacts between the nanowire and electrodes are perfect and their electronic states are identical, the number of conduction channels multiplied by the conductance unit $2e^2/h$ is equal to the conduc-

tance of the perfect-contact system. The conductance values shown in Fig. 2(a) are much smaller than the perfect ones. This result reflects the facts that the electronic states of the Si nanowire and the Au electrodes are different, and their contacts are not good mainly due to the lattice mismatch between them. But, since these spectra are roughly proportional, it is considered that the conductance spectrum in Fig. 2(a) shows features intrinsic to the electronic states of the Si nanowire. We calculated the conductance with shifting the position of the Si nanowire in a direction perpendicular to the wire axis, and verified that the conductance spectrum does not qualitatively depend on the contact position of the Si nanowire on the electrodes. We guess this result due to an averaging effect by lattice mismatch when contact areas are large.

As we will show the band structure of the Si nanowire below, the energy regions below -0.1 eV and above 1.2 eV in the conductance spectrum of Fig. 2(a) correspond to the bulk valence and conduction bands of the nanowire, respectively. The energy regions of the surface-state bands of the Si{111} and {001} surfaces lie between 0.3 and 1.1 eV and between -0.5 and 0.2 eV, respectively. The broad peak near the Fermi energy corresponds to the surface-state bands of the {111} surface. Therefore at low bias voltages current flows mainly through the {111} surfaces of the nanowires, which leads to highly inhomogeneous current distribution.

In order to see this directly we calculate current distribution in the wire. Figure 3 shows current distributions corresponding to the conductances at (a) -0.5, (b) -0.1, (c) 0.6, and (d) 1.0 eV. Current is calculated by the method used in a previous paper.[15] Figures 3(a), 3(b), and 3(c) show the distributions of current carried mainly by the bulk states, {001} surface states, and {111} surface states, respectively. The current distributions of Figs. 3(b) and 3(c) with energies in the bulk band gap are not extended over all the facets of the nanowire but localized on either of the {001} and {111} facets, which reflects the difference in energy regions of the (001) and (111) surface-state bands. Such current distributions localized on individual facets of a nanowire are generally expected, because surface-state bands of different surfaces are generally located in different energy regions. In addition we note that the current distribution in Fig. 3(d) is localized at the edges formed by two {111} surfaces. This result suggests that the current is carried by edge states.

In order to show directly the existence of the edge states we calculate the electronic structure of the isolated Si nanowire. Figure 4 shows the band structure. The densely lined bands below -0.1 eV and above 1.2 eV are the bulk valence and conduction bands, respectively. The band gap of the bulk bands of the nanowire is slightly larger than that of the bulk silicon due to the finite-size effect.[7] In the bulk band gap we see the surface-state bands of the {111} and {001} surfaces. In addition two bands exist: one lies between the {001} and {111} surface-states bands and the other between the {111} surface-state bands and the bulk conduction bands. They are doubly degenerated, corresponding to the existence of the two edges formed by two {111} surfaces. We verified that these bands do not exist in simple superposition of the band structures of the two-dimensional (111) and (001) surfaces.

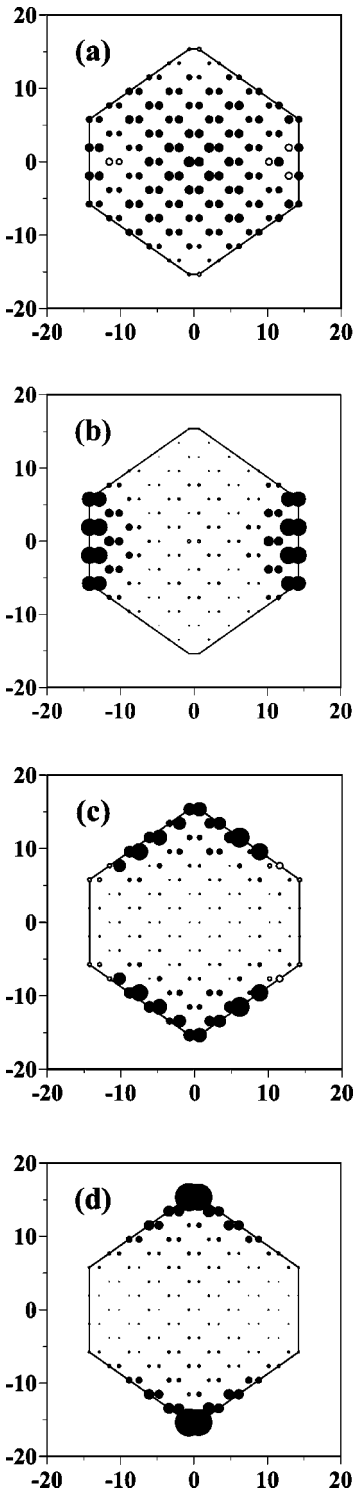

FIG. 3. Current distributions in the Si nanowire. The distributions on the cross sections at the middle two layers of the nanowire are superposed. Energy is (a) -0.5, (b) -0.1, (c) 0.6, and (d) 1.0 eV. Closed and open circles show the currents flowing in the positive and reverse directions along the wire axis, respectively. The radius of the circles is proportional to the absolute value of current. The outermost surface atoms are located on the almost hexagonal octagons. Units of length are Å. These figures show currents carried mainly by (a) bulk states, (b) {001} surface states, (c) {111} surface states, and (d) edge states.

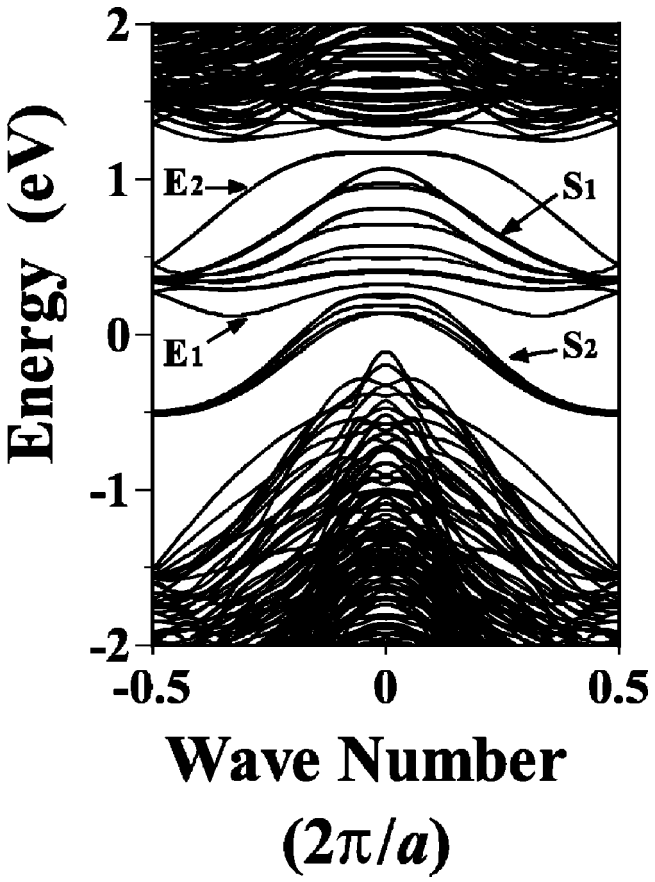

FIG. 4. Band structure of the isolated Si nanowire. S_1 and S_2 indicate the surface-state bands of the {111} and {001} surfaces, respectively. Edge-state bands are labeled by E_1 and E_2. Zero in energy corresponds to the top of the valence bands of bulk silicon, a is the lattice constant of the wire.

Figure 5 shows a wave function of a state in the upper edge band. The wave function is localized at the edges formed by two {111} surfaces. The wave functions in the lower edge band are also localized at the edges of the two {111} surfaces. There is no edge state localized at the edges formed by the {111} and {001} surfaces.

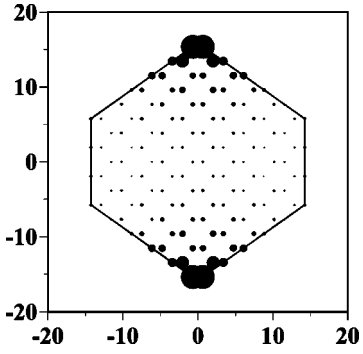

FIG. 5. Wave function of an edge state of the Si nanowire. The distribution shows the state in the E_2 band in Fig. 4 at the center of the Brillouin zone. The radius of the circles is proportional to the squared absolute value of the wave function. Units of length are in Å.

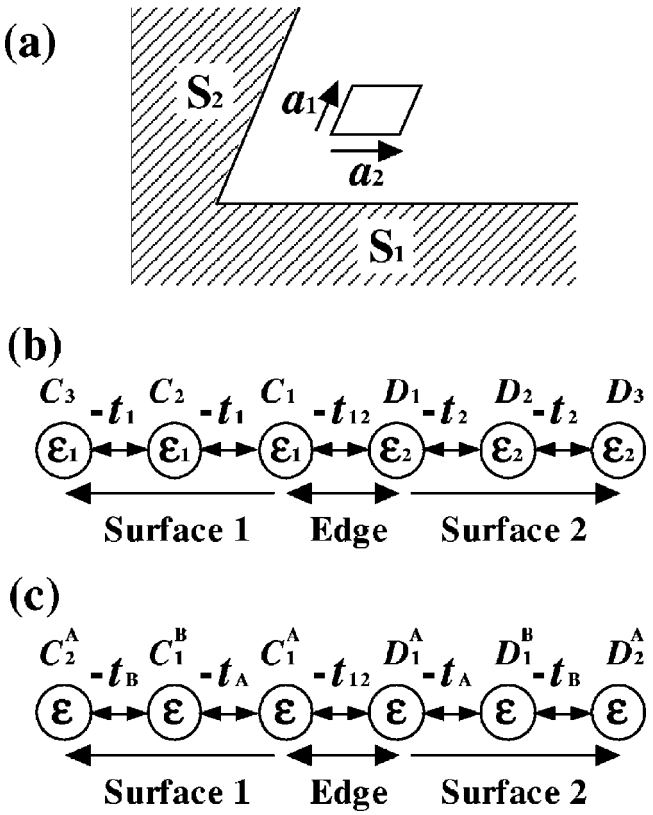

FIG. 6. (a) Cross section of a wedge surrounded by two surfaces S_1 and S_2. The parallelogram shows a unit cell of the wedge. $\mathbf{a}_1$ and $\mathbf{a}_2$ are primitive lattice vectors of the cell. (b), (c) One-dimensional models for edge states. Left and right chains express the two surfaces of the wedge above. The joint of the chains corresponds to the edge region. ε_1 and ε_2 of (b) are the onsite energies of the left and right chains, respectively. $-t_1$ and $-t_2$ are the intrachain transfer energies of the left and right chains, respectively. $-t_{12}$ is the interchain transfer energy. C_n and D_n are coefficients in a wave function at the nth site in the left and right chains numbered from the edge. The parameters of (c) are defined similarly.

We calculate the electronic states of a nanowire with a smaller diameter. The cross section of the wire is smaller than that in Fig. 1(b) by one double layer on each surface. In this case also edge states appear, and the electronic structure is not qualitatively different from those of the larger nanowire.

The numerical results above suggest that the appearance of edge states depends on the combination of the two surfaces intersecting at edges, and there are conditions for the existence of edge states. We discuss the conditions using simple models in the following section.

IV. DISCUSSION OF EDGE STATE

Since the edge states are localized at the edges of nanowires, we can discuss them using a wedge shown in Fig. 6(a) instead of nanowires. The wedge is surrounded by two semi-infinite surfaces labeled as S_1 and S_2. Since they are surfaces of a crystal, the unit cell of the wedge can be defined by two primitive lattice vectors parallel to the cross section of the wedge.

When the angle between the two surfaces is large, the interaction between the surface states localized on each surface is small except for the region near the edge. Therefore we can use a one-dimensional model shown in Fig. 6(b) in order to discuss the existence of the edge states. The left and right chains express the two surfaces of the wedge. The joint of the chains corresponds to the edge. We neglect the atomic structures in the direction along the edge line for simplicity, because it is easy to take account of it by considering one-dimensional Bloch states along the edge direction.

The chain atoms may be regarded as the topmost atoms of the surfaces or more generally the surface regions where surface states are localized. We assume single *s* orbital for each atom. The onsite energies of the orbitals of surface 1 and 2 are ε_1 and ε_2, and their transfer energies are $-t_1$ and $-t_2$, respectively. The transfer energy between the edge atoms of surface 1 and 2 is $-t_{12}$. The coefficients of the orbitals in linear combination of atomic orbitals are C_n and D_n for surface 1 and 2, respectively.

First we consider the symmetrical case where $t_1=t_2\equiv t$ and $\varepsilon_1=\varepsilon_2=0$. When the two surfaces are decoupled ($t_{12}=0$) or we consider independently two infinite surfaces along the directions parallel to the surfaces, the energy E of the surface states is given by

$$E=-2t\cos ka, \tag{4.1}$$

where k and a are a wave number and the lattice constant of the chain. When the two surfaces are coupled at the edge, it is easy to show that if $|t_{12}|>|t|$, two states localized at the edge exist outside the energy region of the surface-state band above. The energies and wave functions of the edge states are given by

$$E=-t\left(\lambda+\frac{1}{\lambda}\right), \tag{4.2}$$

and $C_n=\lambda^{n-1}C_1$, $D_n=\lambda^{n-1}D_1$, and $C_1=\pm D_1$, respectively, where $\lambda=\pm t/t_{12}$. This result explains the edge states formed at the edge of the $(1\bar{1}\bar{1})$ and $(1\bar{1}\bar{1})$ surfaces of the Si nanowire: there are two edge states, and one is below and the other is above the energy region of the surface-state band of the {111} surface.

The edge states with + and − signs in the above may regarded as bonding and antibonding states of the two surface states, respectively. In fact when $|t_{12}|\gg|t|$ the edge states are identical to molecular states of the two atoms at the ends of the left and right surfaces.

The condition $|t_{12}|>|t|$ may not be satisfied in the usual situation that two chains are simply connected, because the interchain interaction is usually weaker than the intrachain one. But this condition may be satisfied at the edges of wedges. For example, as seen from Fig. 1(b) the distance between the dangling bonds of the atoms nearest to the edge of the $(1\bar{1}\bar{1})$ and $(1\bar{1}\bar{1})$ surfaces is shorter than that between the dangling bonds on the {111} surfaces. This suggests that the intersurface interaction of dangling bonds is stronger than the intrasurface one, which leads to the existence of the edge states.

Next we discuss the asymmetrical case. The general conditions for existence of edge states are presented in Appendix A. Here we consider two special cases where the physical meanings of the existence conditions are clear. The first one is that $t_1=t_2\equiv t$ and $\varepsilon_1\neq\varepsilon_2$. The inequality separates the surface-state bands of the two surfaces. In this case also two edge states exist above the upper surface-state band and below the lower one, when $|\alpha|<1$ and $|\Delta\varepsilon/t|<\alpha^2+1/\alpha^2-2$, where $\alpha=t/t_{12}$ and $\Delta\varepsilon=\varepsilon_1-\varepsilon_2$. The former condition is the same as that of the symmetrical case. The latter one means that the surface-states band of the two inequivalent surfaces are not much separated in comparison to the bandwidths. Since α is usually the order of 1, this means that the two surface-state bands overlap. This may explain that no edge state exists at the edges of the {111} and {001} surfaces of the Si nanowire, because the surface-state bands of these surfaces are separated as seen from Fig. 4.

The second special case is that $t_1\neq t_2$ and $\varepsilon_1=\varepsilon_2$. In this case the conditions for existence of edge states are $\alpha^2+1/\beta^2>2$ and $\beta^2+1/\alpha^2>2$ with $|\alpha|<1$ and $|\beta|<1$, where $\alpha=t_1/t_{12}$ and $\beta=t_2/t_{12}$. These conditions mean the intersurface interaction t_{12} is stronger than the intrasurface ones t_1 and t_2 by a certain amount. In this case also two edge states exist above and below the broader band.

For the general case that $t_1\neq t_2$ and $\varepsilon_1\neq\varepsilon_2$, the physical meanings of the conditions are not so simple as those above. But it may qualitatively be concluded that the overlap of the surface-state bands of the two surfaces and the strong perturbation at the edge are important factors for existence of edge states.

The surface structures of real Si nanowires may be reconstructed. For example, the {111} surfaces would be reconstructed in the 2×1 structure if the surface area is not so large than that the 7×7 reconstruction forms. In such a case there are two atoms in the unit cell of the chain and we should consider a model shown in Fig. 6(c). The transfer energies take the values $-t_A$ and $-t_B$ by turns. For simplicity we consider the case that the left and right chains are equivalent and all the onsite energies are the same. In this case also it is possible to show the existence of edge states. The derivation is shown in Appendix B.

Due to the two inequivalent atoms in a unit cell, there are two surface-state bands and a band gap opens between them. When $|t_{12}|>|t_B|$, two edge states exist above the upper band and below the lower band. This is similar to the case of one atom in a unit cell. In addition two edge states exist in the band gap, when $|t_{12}|>|t_B|$ and $|t_A|>|t_B|$ or $|t_{12}|<|t_B|$ and $|t_A|<|t_B|$. The Si(111)2×1 surface has two surface-state bands in the bulk band gap and a band gap opens between them.[9,19,20] Therefore there is possibility that two edge states exist in the surface-state band gap at the edges formed by two {111} surfaces.

We calculate the electronic states of nanowires with various axes and surfaces. Figure 7 shows an example. The axis and surfaces of the wire are the [001] direction and four {100} surfaces, respectively. Figure 7(b) shows the band structure. An edge-state band appears below the surface-state bands of the {100} surfaces. Since there are two dangling bonds in a unit cell of the (100)1×1 surface, they form two

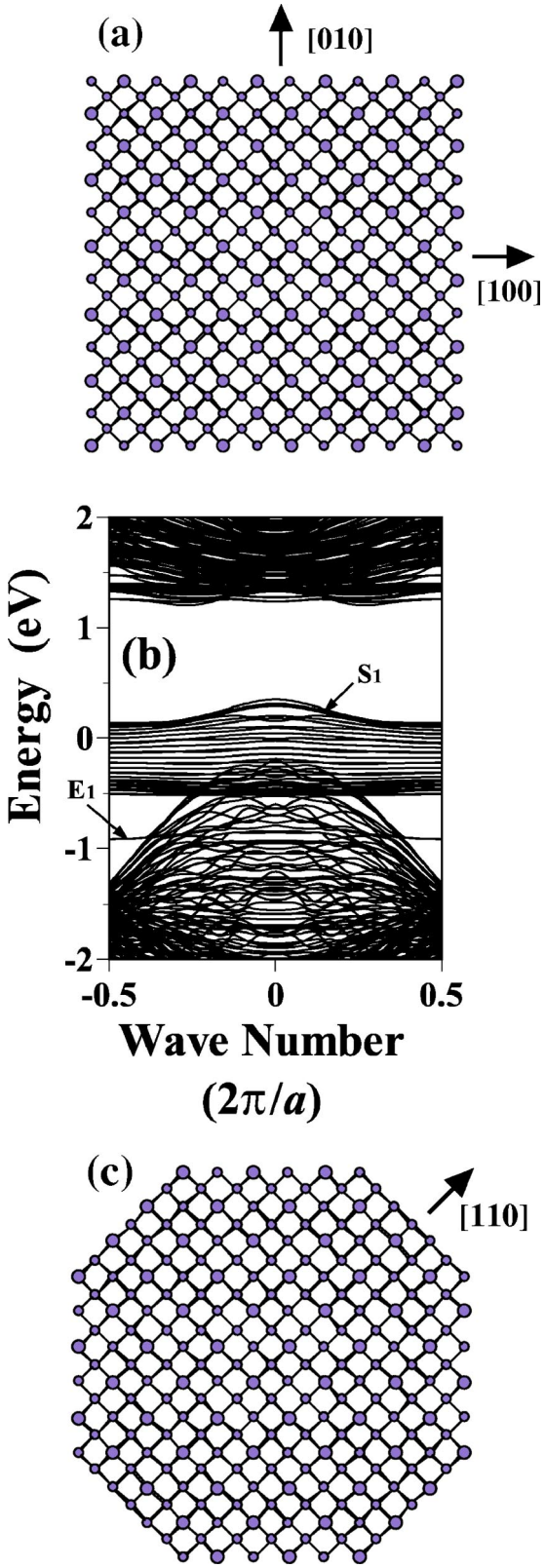

FIG. 7. (a) Cross section and (b) band structure of a Si nanowire with four {100} surfaces. (c) Cross section of a nanowire surrounded by four {100} and {110} surfaces. The wire axis of both the wires is parallel to the [001] direction. S_1 and E_1 in the band structure denote the surface-state bands of the {100} surfaces and the edge-state band, respectively, a is the lattice constant of the wire.

surface-state bands. The surface-state bands shown in Fig. 7(b) are the lower bands. The upper ones are hidden in the energy region of the bulk conduction bands. Therefore the present case corresponds to the model in Fig. 6(c). In fact we verified that there are states localized at the edges of the nanowire above the upper surface-state bands. Edge states are not found in the band gap between the lower and upper surface-state bands in the present case.

When {110} surfaces are introduced to the wire as shown in Fig. 7(c), the edge-state band disappears. This may be due to little overlap of the surface-state bands of the (100) and (110) surfaces. When the nanowire is surrounded by only four {110} surfaces, two edge-state bands appear above and below the surface-state bands of the {110} surfaces, which also corresponds to the model of Fig. 6(a). Detailed analyses of the edge states of various nanowires will be presented in a separate paper.

The edge states of wedges have already be studied in the acoustic phonons of elastic continua[21–23] and the electrostatic modes of dielectric wedges.[24] The image states of an electron bound near a right-angle corner surrounded by two surfaces were also studied theoretically.[25] The edge states in this paper are different from these ones in the point that the present ones are electronic localized states consisting of Shockley-type surface states.

States induced by edges were also found theoretically[26,27] and were observed experimentally[28–34] at steps of surfaces. The edge states of steps may be similar to the present ones in the point that they appear by the violation of translation symmetry of surfaces at edges. Actually there are step states essentially identical to the present edge states. But some step states may be differentiated in the point that the wave functions of the edge states at an intersection of two semi-infinite surfaces decay on both the surfaces with increasing the distances from the intersection. Since the steps usually studied are one or two atomic steps, it is difficult to determine whether the wave function decays or propagates on the riser surface of a step. Therefore, the surface states localized on the riser surface may be regarded as edge states in the case of step edges. They are decaying waves on the terrace but are standing waves on the riser surface.

The present edge states can be classified as follows in the context of complex band structures.[35] An electron wave function in a crystal has properties

$$\psi(\mathbf{r}+\mathbf{a}_i)=\lambda_i\psi(\mathbf{r}), \quad i=1,2,3, \tag{4.3}$$

where $\mathbf{a}_i$ is a primitive translational vector. When $|\lambda_i|=1$ for all i, the state is a bulk state. The surface states localized on the surface S_1 parallel to the two vectors $\mathbf{a}_2$ and $\mathbf{a}_3$ consist of waves with $|\lambda_1|\neq 1$ and $|\lambda_2|=|\lambda_3|=1$. The surface states on the surface S_2 parallel to $\mathbf{a}_1$ and $\mathbf{a}_3$ have similar properties. Therefore the edge states localized at the intersection of these two surfaces S_1 and S_2 are composed of waves with $|\lambda_1|\neq 1$, $|\lambda_2|\neq 1$, and $|\lambda_3|=1$. The pure edge states lie outside the bulk-state bands and the surface-state bands of both the S_1 and S_2 surfaces. This classification leads to the existence of vertex states localized at the intersection of edge lines parallel to the three translational vectors. The vertex

states should be composed of waves with $|\lambda_i| \neq 1$ for all i, and lie outside the bulk-state, surface-state, and edge-state bands. We calculated the electronic state of a Si nanoparticle and verified the existence of vertex states. The details of the vertex states will be presented in a separate paper.

In the present paper we did not self-consistently calculate the electronic states of the system. When we take account of the charge redistribution, following changes are expected. One is the Schottky barrier formation at metal-semiconductor contacts.[5] Since the present medium-sized Si nanowires have partially filled surface states, the surface regions of the nanowires are metallic. This inhomogeneity of the nanowires may make the Schottky barrier more complex than that in the simple metal-semiconductor contacts.

Second is the charge transfer between inequivalent surfaces. As shown in Fig. 4 the surface-state bands of the ideal {111} surface lie above those of the {001} surface. This means that the charge transfer from the {111} surfaces to the {001} surfaces occurs, and the former and latter surfaces are positively and negatively ionized, respectively. The self-consistency lifts and lowers the {001} and {111} surface-state bands, respectively. This mutual approach of the surface-state bands tends toward the appearance of edge states at the edges of the inequivalent surfaces as discussed above.

However, it may be expected that the charge transfer does not occur between the {111} and {001} 2×1 reconstructed surfaces, because the surface-state bands of both surfaces are split into occupied and empty bands, and the Fermi energies of these surfaces do not much differ.[9] In this case edge states may exist without charge transfer, because the surface-state bands of these surfaces overlap.

V. CONCLUSION

We studied the surface-state conduction of medium-sized nanowires. The conductance and electronic states of the ideal Si nanowires with {111} and {100} facets were calculated as an example. The current distributions in the energy region of the bulk band gap are localized at either of the {111} and {100} surfaces, reflecting the difference in the energy regions of these surface-state bands. In addition there are energy regions where currents are carried by the edge states localized at the intersections of two {111} surfaces. These results demonstrate the highly inhomogeneous current distribution in medium-sized nanowires.

The existence conditions of edge states were discussed using the one-dimensional models. Though the conditions vary with the details of surface structures, it may be concluded that the overlap of the surface-state bands of the two surfaces forming a wedge and the strong perturbation at the edge are generally favorable for the existence of edge states. Furthermore we pointed out the possibility of the existence of vertex states.

The inhomogeneous distributions of the currents carried by surface states and edge states may affect other physical properties of medium-sized nanowires. For example, electron-phonon scatterings take place mainly at surfaces or edges and the dissipation of energy is not simple. The temperature distribution is determined by the generation of heat and the heat current conductivity, which also may be not homogeneous. These problems will be discussed in future works.

ACKNOWLEDGMENTS

Numerical calculations were performed at supercomputers at the Institute of Solid State Physics. This work is partially supported by a Grant-in-Aid from the Ministry of Education, Culture, Sports, Science and Technology, Japan.

APPENDIX A

We present the conditions for existence of edge states in the model of Fig. 6(b). We seek solutions in the form of $C_n=\lambda_1^{n-1}C_1$ and $D_n=\lambda_2^{n-1}D_1$ with $|\lambda_1|<1$ and $|\lambda_2|<1$. The tight-binding equations are reduced to

$$E=\varepsilon_1-t_1(\lambda_1+1/\lambda_1), \tag{A1}$$

$$E=\varepsilon_2-t_2(\lambda_2+1/\lambda_2), \tag{A2}$$

$$EC_1=\varepsilon_1C_1-t_1\lambda_1C_1-t_{12}D_1, \tag{A3}$$

and

$$ED_1=\varepsilon_2D_1-t_2\lambda_2D_1-t_{12}C_1. \tag{A4}$$

These equations yield

$$\lambda_1\lambda_2=\alpha\beta, \tag{A5}$$

where $\alpha=t_1/t_{12}$ and $\beta=t_2/t_{12}$. Therefore the condition $|\alpha\beta|<1$ is necessary. From Eqs. (A1) and (A2) we obtain

$$\left(\frac{1}{\alpha}-\alpha\right)\lambda_1-\left(\frac{1}{\beta}-\beta\right)\lambda_2+\frac{\Delta\varepsilon}{t_{12}}=0 \tag{A6}$$

where $\Delta\varepsilon=\varepsilon_1-\varepsilon_2$. The condition for existence of edge states is that the curves in Eqs. (A5) and (A6) have points of intersection in the region $|\lambda_1|<1$ and $|\lambda_2|<1$ on the λ_1-λ_2 plane.

The conditions for the case that there is one solution in the region $|\alpha\beta|<\lambda_1<1$ or $-1<\lambda_1<-|\alpha\beta|$ are

$$-\gamma<\Delta\varepsilon<\delta, \tag{A7}$$

or

$$-\delta<\Delta\varepsilon<\gamma, \tag{A8}$$

where $\gamma=|t_2|(\alpha^2+1/\beta^2-2)$ and $\delta=|t_1|(\beta^2+1/\alpha^2-2)$. It can be proved that it is impossible that two solutions exist in either region above.

APPENDIX B

We show that edge states exist in the model of Fig. 6(c). We seek solutions in the form of $C_n^{\mathrm{A}}=\lambda^{n-1}C_1^{\mathrm{A}}$ and $C_n^{\mathrm{B}}=\lambda^{n-1}C_1^{\mathrm{B}}$ with $|\lambda|<1$. Since the system is symmetrical about the center, we may choose that $D_n^{\mathrm{A}}=\pm C_n^{\mathrm{A}}$ and $D_n^{\mathrm{B}}=\pm C_n^{\mathrm{B}}$. The tight-binding equations are reduced to

$$EC_1^{\mathrm{A}}=-t_{\mathrm{A}}C_1^{\mathrm{B}}-\frac{t_{\mathrm{B}}}{\lambda}C_1^{\mathrm{B}}, \tag{B1}$$

$$EC_1^{\mathrm{B}} = -t_{\mathrm{A}}C_1^{\mathrm{A}} - t_{\mathrm{B}}\lambda C_1^{\mathrm{A}}, \tag{B2}$$

and

$$EC_1^{\mathrm{A}} = -t_{\mathrm{A}}C_1^{\mathrm{B}} - t_{12}(\pm C_1^{\mathrm{A}}), \tag{B3}$$

where we choose the origin of energy at the onsite energy ε. The first two equations above yield

$$E^2 = t_{\mathrm{A}}^2 + t_{\mathrm{B}}^2 + t_{\mathrm{A}}t_{\mathrm{B}}\left(\lambda + \frac{1}{\lambda}\right), \tag{B4}$$

and the first and third equations yield

$$\lambda = \pm\frac{t_{\mathrm{B}}}{t_{12}}\frac{C_1^{\mathrm{B}}}{C_1^{\mathrm{A}}}. \tag{B5}$$

This equation combined with Eqs. (B1) and (B2) yields a quadratic equation in λ

$$\lambda^2 + p(1-q^2)\lambda - q^2 = 0, \tag{B6}$$

where $p = t_{\mathrm{B}}/t_{\mathrm{A}}$ and $q = t_{\mathrm{B}}/t_{12}$. Here we define that $f(x) = x^2 + p(1-q^2)x - q^2$. Since $f(0) = -q^2 < 0$ and $f(\pm 1) = (1 \pm p)(1-q^2)$, a necessary condition for the existence of solutions with $|\lambda| < 1$ is that $(1+p)(1-q^2) > 0$ or $(1-p)(1-q^2) > 0$. In addition, for real energy E to exist, the right side of Eq. (B4) must not be negative when the solutions of Eq. (B6) are substituted into it. These are the sufficient conditions for the existence of the edge states.

Since Eq. (B4) can be rewritten as

$$\left(\frac{E}{t_{\mathrm{A}}}\right)^2 = 1 + p^2 + p\left(\lambda + \frac{1}{\lambda}\right), \tag{B7}$$

the solution λ with $p\lambda > 0$ exists if $q^2 < 1$. There are two edge states for this solution. One is located in energy above the upper surface-state band and the other below the lower one.

The solution with $p\lambda < 0$ exists when $|p| < 1$ and $q^2 < 1$, or $|p| > 1$ and $q^2 > 1$. This result comes from an inequality

$$f(-p)f(-1/p) = -\frac{q^2}{p^2}(1-p^2)^2 < 0. \tag{B8}$$

This means that the solution λ exists between $-p$ and $-1/p$ and we obtain

$$\frac{p}{\lambda}(\lambda + p)(\lambda + 1/p) > 0, \tag{B9}$$

which is equivalent to that the right side in Eq. (B7) is positive. In this case also there are two edge states which are located in the band gap between the two surface-state bands.

[1] C.J. Fall, N. Binggeli, and A. Baldereschi, Phys. Rev. Lett. **88**, 156802 (2002).
[2] C.J. Fall, N. Binggeli, and A. Baldereschi, Phys. Rev. B **66**, 075405 (2002).
[3] A.S. Barnard, S.P. Russo, and I.K. Snook, Surf. Sci. **538**, 204 (2003).
[4] B. Marsen and K. Sattler, Phys. Rev. B **60**, 11 593 (1999).
[5] U. Landman, R.N. Barnett, A.G. Scherbakov, and P. Avouris, Phys. Rev. Lett. **85**, 1958 (2000).
[6] B. Li, P. Cao, R.Q. Zhang, and S.T. Lee, Phys. Rev. B **65**, 125305 (2002).
[7] D.D.D. Ma, C.S. Lee, F.C.K. Au, S.Y. Tong, and S.T. Lee, Nature (London) **299**, 1874 (2003).
[8] Y. Zhao and B.I. Yakobson, Phys. Rev. Lett. **91**, 035501 (2003).
[9] A.A. Stekolnikov, J. Furthmuller, and F. Bechstedt, Phys. Rev. B **65**, 115318 (2002).
[10] P. Vogl, H.P. Hjalmarson, and J.D. Dow, J. Phys. Chem. Solids **44**, 365 (1983).
[11] W.A. Harrison, *Elementary Electronic Structure* (World Scientific, Singapore, 1999).
[12] R. Landauer, IBM J. Res. Dev. **1**, 223 (1957).
[13] M. Büttiker, Y. Imry, R. Landauer, and S. Pinhas, Phys. Rev. B **31**, 6207 (1985).
[14] Y. Imry and R. Landauer, Rev. Mod. Phys. **71**, S306 (1999).
[15] K. Kobayashi, Phys. Rev. B **65**, 035419 (2002).
[16] K. Kobayashi, Phys. Rev. B **66**, 085413 (2002).
[17] K. Kobayashi and E. Ishikawa, Surf. Sci. **540**, 431 (2003).
[18] K. Kobayashi, Phys. Rev. B **68**, 075308 (2003).
[19] J.E. Northrup, M.S. Hybertsen, and S.G. Louie, Phys. Rev. Lett. **66**, 500 (1991).
[20] M. Rohlfing and S.G. Louie, Phys. Rev. Lett. **83**, 856 (1999).
[21] A.A. Maradudin, R.F. Wallis, D.L. Mills, and R.L. Ballard, Phys. Rev. B **6**, 1106 (1972).
[22] S.L. Moss, A.A. Maradudin, and S.L. Cunningham, Phys. Rev. B **8**, 2999 (1973).
[23] T.M. Sharon, A.A. Maradudin, and S.L. Cunningham, Phys. Rev. B **8**, 6024 (1973).
[24] L. Dobrzynski and A.A. Maradudin, Phys. Rev. B **6**, 3810 (1972).
[25] W.W. Lee and P.R. Antoniewicz, Phys. Rev. B **40**, 3352 (1989).
[26] M. Schlüter, K.M. Ho, and M.L. Cohen, Phys. Rev. B **14**, 550 (1976).
[27] M.C. Desjonquères and F. Cryrot-Lackmann, Solid State Commun. **18**, 1127 (1976).
[28] J.F. van der Veen, D.E. Eastman, A.M. Bradshaw, and S. Holloway, Solid State Commun. **39**, 1301 (1981).
[29] H. Namba, N. Nakanishi, T. Yamaguchi, and H. Kuroda, Phys. Rev. Lett. **71**, 4027 (1993).
[30] Ph. Avouris and I.-W. Lyo, Science **264**, 942 (1994).
[31] J.E. Ortega, F.J. Himpsel, R. Haight, and D.R. Peale, Phys. Rev. B **49**, 13 859 (1994).
[32] X.Y. Wang, X.J. Shen, and R.M. Osgood, Jr., Phys. Rev. B **56**, 7665 (1997).
[33] X.J. Shen, H. Kwak, D. Mocuta, A.M. Radojevic, S. Smadici, and R.M. Osgood, Jr., Phys. Rev. B **63**, 165403 (2001).
[34] L. Bartels, S.W. Hla, A. Kühnle, G. Meyer, K.-H. Rieder, and J.R. Manson, Phys. Rev. B **67**, 205416 (2003).
[35] V. Heine, Proc. Phys. Soc. London **81**, 300 (1963).